Radio Instrument Package for Lunar Ionospheric Observation: A Concept Study

C. Watson[1], P. T. Jayachandran[1], A. Kashcheyev[1], D. R. Themens[1,2], R. B. Langley[3], R. Marchand[4], A. W. Yau[5]

[1]University of New Brunswick, Physics Department, Fredericton, NB, Canada.

[2]University of Birmingham, Space Environment and Radio Engineering (SERENE) Group, School of Engineering, Birmingham, UK.

[3]University of New Brunswick, Department of Geodesy and Geomatics Engineering, Fredericton, NB, Canada

[4]University of Alberta, Department of Physics, Edmonton, AB, Canada

[5]University of Calgary, Department of Physics and Astronomy, Calgary, AB, Canada

Corresponding author: Chris Watson (chris.watson@unb.ca)

Key Points:

- We propose a "crosslink" radio occultation method of observing electrically charged constituents of the lunar exosphere
- Simulations demonstrate that two CubeSats in lunar orbit result in a substantial increase in lunar ionosphere observational capacity
- We demonstrate that a VHF transmitter-receiver "crosslink" setup is ideal for making radio occultation observations of the lunar ionosphere

Abstract

The lunar ionosphere is a ~100 km thick layer of electrically charged plasma surrounding the moon. Despite knowledge of its existence for decades, the structure and dynamics of the lunar plasma remain a mystery due to lack of consistent observational capacity. An enhanced observational picture of the lunar ionosphere and improved understanding of its formation/loss mechanisms is critical for understanding the lunar environment as a whole and assessing potential safety and economic hazards associated with lunar exploration and habitation. To address the high priority need for observations of the electrically charged constituents near the lunar surface, we introduce a concept study for the Radio Instrument Package for Lunar Ionospheric Observation (RIPLIO). RIPLIO would consist of a multi-CubeSat constellation (at least two satellites) in lunar orbit for the purpose of conducting "crosslink" radio occultation measurements of the lunar ionosphere, with at least one satellite carrying a very high frequency (VHF) transmitter broadcasting at multiple frequencies, and at least one satellite flying a broadband receiver to monitor transmitting satellites. Radio occultations intermittently occur when satellite-to-satellite signals cross through the lunar ionosphere, and the resulting phase perturbations of VHF signals may be analyzed to infer the ionosphere electron content and high- resolution vertical electron density profiles. As demonstrated in this study, RIPLIO would provide a novel means for lunar observation, with the potential to provide long-term, high-resolution observations of the lunar ionosphere with unprecedented pan-lunar detail.

Plain Language Summary

The lunar ionosphere comprises electrically charged particles within the lunar atmosphere and is derived from a wide range of sources and formation mechanisms that are not fully resolved. Although extremely tenuous compared to that of Earth's, the lunar ionosphere plays an integral role in physical processes occurring within the lunar environment. The composition and dynamics of the lunar ionosphere are mostly unknown at this point and may be linked to the lunar surface and sub-surface, solar wind, magnetosphere, and Earth's atmosphere. Observation of the lunar ionosphere is essential to develop a complete picture of its structure and dynamic behaviour and how it is formed. This is a critical aspect of assessing its physical role within the lunar environment and potential safety hazards for future lunar exploration and habitation. This paper presents the concept of a radio-based mission for lunar ionospheric observation called the Radio Instrument Package for Lunar Ionospheric Observation (RIPLIO). This mission would employ multiple CubeSats in lunar orbit, equipped with radio transmitters and receivers, to observe the lunar ionosphere with unprecedented detail. This paper presents preliminary simulations of radio measurements of the lunar ionosphere, and discusses requirements for a potential RIPLIO mission and relevance to international science objectives.

1. Introduction

The lunar atmosphere, also considered an "exosphere," consists of a gravitationally-bound, tenuous, collisionless gas, thought to be dominated by inert atoms (e.g. Ar, Ne, and He) or dust with densities on the order of 10^4-10^5 cm^{-3} [*Stern,* 1999 and references within]. Exospheric constituents mainly originate from the lunar regolith and subsurface, the solar wind, and micrometeorites. This thin (10s of kilometers) atmospheric layer is an integral part of a highly coupled system comprising the lunar environment, sun, and solar system, and was identified as one of eight key areas of focus for lunar science by the United States National Research Council in "The Scientific Context for Exploration of the Moon" [*NRC*, 2007]. This document also emphasized the importance of promptly observing the native lunar atmosphere, as the anticipated increase in human activity will disrupt this fragile environment and impede the study of its structure, dynamics, and formation mechanisms in its pristine state.

The presence of a lunar ionosphere, the electrically charged constituents of the lunar atmosphere, was first inferred from lunar refraction of signals originating form astronomical objects that occulted the lunar limb, which provided lunar electron density estimates of up to 1000 cm^{-3} [*Elsmore,* 1957; *Andrew et al.,* 1964]. The first direct observational evidence of a lunar ionosphere was provided by observations of the Charged Particle Lunar Environment Experiment (CPLEE) ion-electron spectrometer and three Suprathermal Ion Detector Experiment (SIDE) mass spectrometers installed on the lunar surface during the Apollo missions in late 1969 and the early 1970s [*Lindeman et al.,* 1973; Benson *et al.,* 1975]. Since the Apollo era, satellite radio occultation (RO) measurements have been a prevalent tool for observing the lunar ionosphere. To date, the lunar RO technique has primarily employed radio sounding using an Earth-based ground station to monitor satellite-to-Earth radio transmissions as the signal path moves in the vicinity of the lunar limb. Observed phase perturbations in the received signal may be attributed to refractive effects of lunar ionosphere plasma (after removal of the terrestrial ionospheric effects), from which the columnar electron content along the signal path and density of the lunar ionospheric plasma can be inferred. The first lunar RO measurements of the Pioneer 7 probe suggested the presence of lunar ionosphere plasma with densities not exceeding 40 cm^{-3} [*Pomalaza-Diaz,* 1967]. Luna 19 and 22 spacecraft were used to conduct dual frequency RO measurements, detecting electron densities of 500-1000 cm^{-3} [*Vasil'ev et al.,* 1974; *Vyshlov and Savich*, 1979]. The Istituto di Radioastronomia of the Istituto Nazionale di Astrofisica conducted lunar occultation campaigns in 2006-2007 using radio telescopes to observe signals of SMART-1, Cassini, and Venus Express as they occulted the lunar ionosphere, with estimated lunar ionosphere columnar electron content of ~10^{13} m^{-2} said to be "in agreement" with results of the Luna mission [*Pluchino et al.,* 2008]. The SELenological and Engineering Explorer (SELENE; aka Kaguya) mission [*Imamura et al.,* 2008; *Imamura et al.,* 2010] used dual frequency transmissions to observe only a fraction of the electron content observed by Luna, possibly due to either lower solar activity levels comparted to the Luna observation period or the polar observation of SELENE as opposed to lower latitude observations of Luna [*Ando et al.,* 2012]. As the primary error source in satellite-to-Earth RO links arises from variations in the Earth's ionosphere, SELENE also employed dual-satellite observations to alleviate some of this error, where one spacecraft at lunar limb-viewing configuration, with a second spacecraft situated away from the limb monitoring the interplanetary and terrestrial plasma.

A second experiment of SELENE used for lunar ionospheric detection was the Lunar Radar Sounder (LRS), which observed auroral kilometric radiation (AKR; 100-500 kHz) of Earth origin. Phase perturbations of AKR signals due to propagation through the lunar ionosphere were used to determine electron content and reconstruct lunar ionosphere density profiles [*Ono et al.,* 2010]. Based on these measurements, *Goto et al.* [2011] inferred lunar ionosphere electron densities on the order of 10s of electrons/cm^3, again substantially smaller than observed by Luna. *Choudhary et al.* [2016] presented a lunar electron density profile based on measurements of a July 2009 radio occultation of the Chandrayaan-1 satellite, which showed electron densities in the range of 100s of electrons/cm^{-3} extending up to ~40 km above the lunar surface.

While the existence of the lunar ionosphere has been established for decades, its structure, dynamic behaviour, and formation mechanisms remain unresolved due to extremely limited observational capacity and the significant discrepancies in existing results. Neutral atmospheric constituents may be ionized through photoionization by solar radiation, energetic particle impacts, or charge exchange reactions, while ions may sputter directly from the lunar surface due to direct impacts of solar wind plasma [*Stern,* 1999; *Sarantos et al.,* 2012]. However, the electric field induced on the lunar surface by the interplanetary magnetic field (IMF) tends to sweep ionized constituents away from the lunar region, limiting the accumulation of lunar-derived ions to densities below the ambient solar wind plasma density [*Johnson*, 1971; *Hodges et al.,* 1974; *Stern,* 1999]. High energy "pick-up ions" of lunar origin, swept away from the lunar atmosphere by the solar wind, have been

observed downstream of the Moon [*Halekas et al.* 2012, 2013, 2015; *Poppe et al.,* 2016].

The Moon spends ~4-6 days of its ~27-day orbit in the Earth's magnetotail, during which the lunar ionosphere interacts with the Earth's magnetospheric plasma environment rather than the solar wind and IMF. Lunar ionospheric structure and dynamic behaviour is modified during this period of "magnetospheric shielding" from the solar wind, and may include encounters with the highly variable and hot plasma of the magnetospheric plasma sheet. The magnetosphere interactions can result in more extreme charge accumulations on the lunar surface, modifying the electrodynamics and plasma constituents of the lunar environment [*Stubbs et al.*, 2007; *Poppe et al.,* 2012; *Zhou et al.,* 2013]. *Halekas et al.* [2018] used plasma oscillations of the ARTEMIS electric field instrument to infer enhanced lunar ionosphere plasma densities on the dayside of the Moon within the geomagnetic tail.

Several alternative mechanisms have been proposed to account for lunar ionosphere densities as large as 1000 cm^{-3}. An increase in release of Ar and Ne from the lunar surface around the solar terminator has been suggested as a possible source of localized plasma density enhancement [*Hodges et al.,* 1974; *Daily et al.,* 1977]. Enhanced lunar crustal magnetic fields observed by Apollo missions [*Lin et al.,* 1998] may trap the ionized constituents in a "mini-magnetosphere" configuration, preventing localized lunar ionosphere regions from being swept away [*Savich,* 1976]. In addition, photo and secondary electron emissions from exospheric dust particles (i.e., "dusty plasma") have been suggested to comprise a significant and potentially dominant portion of the lunar ionosphere [*Stubbs et al.*, 2011] where dust particles are accelerated upwards from the lunar surface by local electric fields, micrometeor impacts, and artificial sources (e.g., lunar landers) and subsequently ionized by solar UV radiation [*Stubbs et al.,* 2006]. The Lunar Prospector satellite has observed significantly enhanced electric potentials on the dark lunar surface [*Halekas et al.,* 2008], which may contribute to enhanced uplift of lunar dust on the far side and polar regions of the Moon. The possibility of the lunar ionosphere consisting primarily of ionized dust is intriguing, as the planetary ionospheres observed and studied thus far consist of an ionized gas. The dynamics and structure of an ionized dust medium are largely open questions, as are the potential effects of dusty plasma on radio communication systems and navigation capabilities during future lunar missions. Additional possible sources of lunar ionospheric plasma are the solar wind plasma itself, or the continuous loss of Earth's ionospheric constituents to the magnetosphere, which may be inserted into the lunar environment during the Moon's passage through the Earth's magnetotail. Given the potential variety of lunar ionosphere formation mechanisms that can occur over a broad range of temporal and spatial scales, a complete observational picture of the lunar ionosphere and understanding of how it is formed requires a large quantity of high temporal and spatial resolution observations on a global (pan-lunar) scale.

Attaining a thorough observational picture of the lunar ionosphere, better understanding of the physical mechanisms governing the formation and loss of ionospheric plasma, and a predictive understanding of lunar ionospheric behaviour is considered a high priority concern for future lunar exploration and habitation for a number of reasons: (1) The lunar ionospheric plasma is quite different from that of Earth's, potentially consisting of dusty plasma and ionized inert gases, and its effects on radio communication and navigation systems operating in the lunar environment are largely unknown; (2) The ionosphere (including dusty plasma) is a safety hazard for humans and satellite/surface equipment during lunar missions, with the potential to damage spacesuits, charge electronics, and clog machinery; (3) The lunar ionosphere is intimately linked to electrodynamic processes occurring within the near-moon environment, as well as processes and constituents characteristic of the lunar surface and interior (e.g. moonquakes, radiation seepage, meteor impacts), and thus a thorough understanding of the lunar ionosphere is essential for understanding the lunar environment as a whole.

Here we introduce the concept of a crosslink RO system to make unprecedented, long-term observations of the lunar ionosphere. The long-term scientific objectives of a crosslink lunar RO mission would be: (1) To provide global, high-resolution vertical electron density profiles of the lunar ionosphere; (2) To observe and map the global structure of the lunar ionosphere, including its climatological and transient behaviour under a broad range of solar wind and magnetospheric conditions; (3) To better understand the mechanisms governing the formation, loss, and dynamic behaviour of the lunar ionosphere; and (4) To enhance understanding of the interactions between the Moon's ionosphere and the Earth's magnetosphere and explore the role of magnetospheric shielding on the lunar ionospheric structure and dynamics. In this paper we provide a description of the lunar crosslink RO technique, followed by an orbital assessment and potential quantity and distribution of RO observations, and finally a simulation of an RO event to assess the potential working frequency range of a lunar crosslink RO system. Crosslink RO measurements of the Earth's atmosphere and ionosphere are routinely conducted by using receivers onboard low-Earth orbiting satellites such as COSMIC and CHAMP to observe perturbations of global navigation satellite system (GNSS) transmissions. Crosslink RO measurements of a planetary ionosphere (other than that of Earth's) have been previously conducted by using ultra-high frequency (UHF) transceivers on board the Mars Odyssey (ODY) satellite and Mars Reconnaissance Orbiter (MRO) [*Ao et al.,* 2015; *Asmar et al.,* 2016].

2. Description of the Crosslink RO Technique

Our current knowledge of the vertical distribution of lunar ionosphere electron density is based on very limited RO experiments of various missions [e.g., *Vyshlov*, 1976; *Pluchino et al.*, 2008; *Imamura et al.*, 2012; and *Choudhary et al.*, 2016], which have cumulatively resulted in a few hundred RO observations. Only a small fraction of these observations have resulted in detection of lunar ionospheric constituents. It is unknown whether low detection rates result from a lack of lunar ionospheric presence or difficulty in extracting effects of the tenuous lunar ionosphere from satellite-to-Earth RO observations. There are extensive open questions pertaining to the structure, formation, and dynamic behaviour of the lunar ionosphere, as well as its role in plasma and electrodynamic processes in the near-Moon and magnetospheric environment. These questions can only be addressed through observational campaigns.

Radio occultation is a technique to obtain information about the vertical gradient of the atmospheric refractive index, which is in turn related to the electron density. Radio waves propagating through a medium with free electrons (e.g., an ionosphere) experience refractive effects, which modify the wave's velocity and direction of travel. To first order, the amount of this delay is proportional to the integrated number of free electrons along the signal ray path, often referred to as total electron content (TEC); therefore it is possible to estimate TEC along a particular propagation path by using a linear combination of the received phases of signals at different frequencies, often referred to as the geometry-free linear combination [*Brunini et al.*, 2004; *Jakowski,* 2017].

In the case of planetary/lunar ionospheres, crosslink radio occultations occur when the signal between a transmitting satellite and a second receiving satellite crosses through the ionosphere, which allows for sampling of the ionospheric TEC over a range of altitudes as the occultation event evolves. By applying inversion techniques to RO TEC measurements, such as the standard Abel method [*Abel,* 1826; *Hajj and Romans*, 1998; *Schreiner et al.*, 1999; *Mousa and Tsuda,* 2004], it is possible to reconstruct the vertical electron density profile of the ionosphere.

Here we introduce the concept of a lunar RO system that would employ a satellite-to-satellite "crosslink" configuration to observe the lunar ionosphere. Future work beyond this concept study will assess detailed mission/system requirements for placing two or more CubeSats in lunar orbit; at least one satellite with an onboard multi-frequency radio transmitter, and at least one satellite with a

broadband radio receiver; to conduct RO measurements of the lunar ionosphere and retrieve high-resolution vertical electron density profiles. Whereas Moon-Earth radio occultation links applied in past missions such as Luna and SELENE result in two occultation events (ingress and egress) per satellite pass with highly restricted coverage in latitude and longitude, radio occultation satellite-to-satellite "crosslinks" using multiple spacecraft in orbit around the Moon would benefit from much more frequent occultation events, global coverage, higher vertical resolution, and much higher signal-to-noise ratios (compared to Moon-Earth RO links). As the structure and three-dimensional flows of the lunar ionosphere vary over a broad range of time and spatial scales associated with factors such as sunlight/darkness, interaction of the lunar environment with the solar wind or Earth's magnetosphere, and variability of the lunar surface/interior constituents and electrodynamics, crosslink RO measurements will enable development of a statistical global climatological picture of the lunar ionosphere under a broad range of conditions, which is not attainable using Moon-Earth RO links. This is a critical aspect for a predictive understanding of lunar ionospheric behaviour. Crosslink occultations also eliminate the most serious source of error impacting previous lunar RO missions, which are density fluctuations of the Earth's ionosphere.

Figure 1 illustrates an example of a crosslink radio occultation of the lunar ionosphere for a two-satellite constellation, where the satellite-to-satellite signal paths sample a range of ionospheric altitudes as the satellites progress in their orbits. Occultation tangent points are indicated by red dots. Conceptually, the transmitter would broadcast at two frequencies in the very high frequency (VHF) range, while the broad-band receiver would track the signals and measure the relative phase delays (advances) introduced by the ionospheric medium. This approach has been widely used by the scientific community for sensing the Earth's ionosphere using signals from global navigation satellite systems [e.g., *Komjathy and Langley,* 1996; *Hernandez-Pajares et al.*, 2009; *Jakowski et al.*, 2017; *Watson et al.,* 2018a,b; *Perry et al.*, 2019].

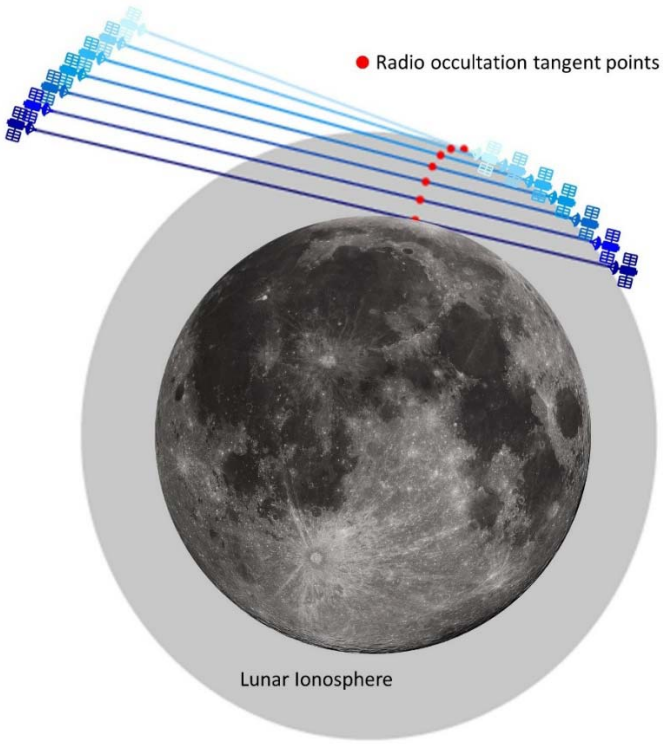

Figure 1. Illustration of a crosslink radio occultation of the lunar ionosphere.

The first successful RO crosslink measurements of a planetary ionosphere (other than Earth) were conducted by using ultra-high frequency (UHF) transceivers on board ODY and MRO spacecraft [*Ao et al.,* 2015; *Asmar et al.,* 2016]. By inverting the residual Doppler of ODY transmissions recorded by MRO, after removal of the modeled expected Doppler due to relative satellite motion, *Ao et al.,* [2015] were able to retrieve Martian ionospheric refractivity and plasma density profiles during three crosslink RO events. *Asmar et al.* [2016] showed that the dual-satellite crosslink technique resulted in thousands of occultations of the Martian ionosphere with dense global coverage after just two weeks, while the single satellite-to-Earth RO link resulted in a fraction of the same coverage in a time span of years. The potential lunar coverage of RIPLIO occultations is discussed in Section 3.

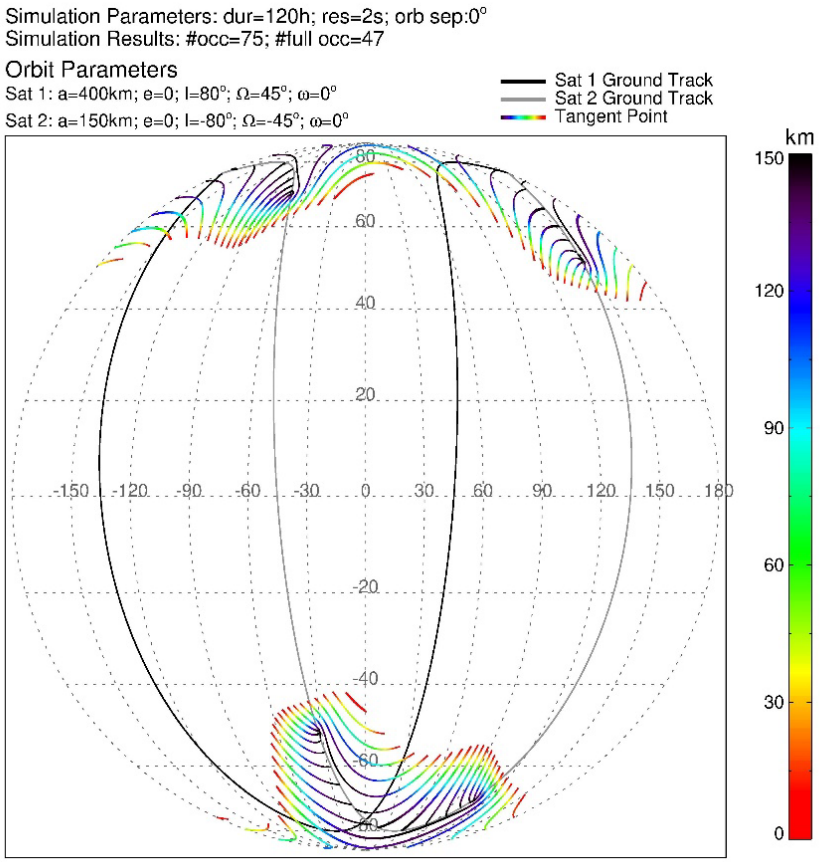

Figure 2. Simulated lunar radio occultations for dual satellite crosslinks over a 120-hour period, for the specified orbital elements.

3. Lunar RO Simulations

Figures 2 and 3 show example simulations of dual-spacecraft "crosslink" lunar occultations over a period of 120 hours, where black and grey lines are satellite ground track coordinates (selenographic), and colored lines show occultation tangent point coordinates, color indicating tangent point altitude. Satellite orbital configurations are specified by orbital elements: altitude (a),

eccentricity (e), inclination (I), longitude of ascending node (Ω), and argument of periapsis (ω). The simulation in Figure 2 demonstrates circular orbits at altitudes of 1000 km and 150 km above the lunar surface, while Figure 3 is for circular orbits at altitudes of 400 km and 150 km. Orbital elements may be tuned to produce a broad range of occultation configurations to fit desired measurement/science objectives, including occultations concentrated at latitudinal/longitudinal regions of interest, or occultations covering a more global scale. The simulation shown in Figure 2 results in 164 complete occultations of the lunar ionosphere spanning a broad range of latitudes and both far and near side of the Moon, while the orbital elements used in the Figure 3 simulation results in 47 complete RO measurements primarily in the polar regions. Each complete RO measurement (ground to Satellite 2 altitude) can be used to produce a complete vertical electron density profile via iterative techniques such Abel inversion. The bold tangent point indicated with an arrow in Figure 2 is used for simulating an RO measurement of a model lunar ionosphere, results of which are shown in Figure 4. Occultation durations listed (in minutes) beside each occultation event in Figures 2 and 3 range from 6.7 to 27.7 minutes, with the bulk of durations below 10.0 minutes. With 1 Hz resolution RO measurements, this corresponds to altitude resolutions ranging from ~0.2 km to ~12 km for vertical electron density profiles. Resolutions are altitude-dependent as the transverse velocity of the occulting signal relative to the lunar surface varies with time.

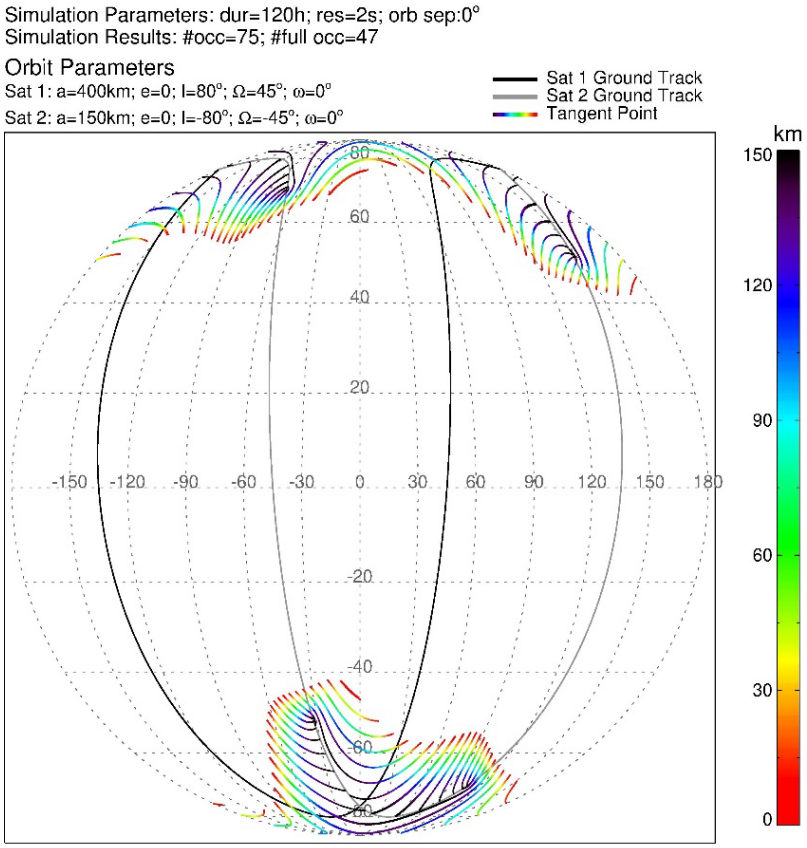

Figure 3. Simulated lunar radio occultations for dual satellite crosslinks over a 120-hour period, for the specified orbital elements.

As a simple example of a lunar crosslink RO simulation, the RO event highlighted by an arrow in Figure 2 is applied to a model ionosphere with spherical symmetry and vertical distribution of the form:

$$N_e(h) = N_{e0} \exp\left[-\left(\frac{h}{H} \right)^{\nu} \right] \quad (1)$$

where N_e is the electron density at altitude h above the lunar surface, N_{e0} is the electron density at the lunar surface, H is a scaling height that governs the rate of decrease in electron density with altitude, and υ is a dimensionless parameter. For a reasonable fit to RO measurements of the Luna 19 spacecraft presented in *Stubbs et al.* (2011), model parameters are set as N_{e0} = 9.5e8 m^{-3}, H = 25 km, and υ = 3, which is referred to as the "Luna 19 fit". Figure 4 shows results of the simulation, where panel (a) is the vertical electron density model, panel (b) is the line-of-site (LOS) TEC as a function of tangent point altitude, where LOS TEC is the electron density integrated along the occulting transmitter-to-receiver signal path:

$$LOS\ TEC = \int N_e dl \quad (2)$$

Panel (c) is the phase advance ($\Delta\Phi$; in units of meters) arising from the electron content shown in (b), for several trial frequencies in the VHF band, calculated using the work of *Appleton* [1932]:

$$\Delta\Phi_i = \frac{e^2}{8\pi^2 \varepsilon_0 m_e f_i^2} LOS\ TEC + \varepsilon_i \quad (3)$$

where e is the electron charge, m_e is the electron mass, ε_0 is the vacuum permittivity, f_i is the ith frequency, and ε_i is the sum of non-ionospheric effects such as Doppler frequency uncertainty and frequency drifts of the onboard oscillator. The term ε_i is set to zero for calculated values shown in (c). Panel (d) is the linear combination of phase perturbations (differential phase, in wave cycles with respect to the lower frequency) for selected frequency pairs. Effects included in ε_i such as clock drift and hardware delays will have to be accounted for in real measurement scenarios. VHF frequencies show a significant response to the model lunar electron content, with frequency-dependent phase advances ranging from ~0.2 m to ~25 m at ground level, and from ~0.01 m to ~1 m at 35 km altitude, where the electron density is an order of magnitude smaller. Corresponding differential phases shown in panel (d) range from ~0.008 to ~0.2 wave cycles at ground level, and from ~0.0001 to ~0.008 cycles at 35 km. Lunar RO TEC of Luna 19 and 22 were derived from differential phases on the order of ~0.04 cycles at S-band frequencies, while SELENE lunar RO TEC was derived from differential phases on the order of ~0.001 cycles at S-band frequencies [*Ando et al.,* 2012]. Larger frequency separations are evidently ideal, even more so since TEC measurements based on larger frequency separations are less sensitive to measurement noise. *Ando et al.* [2012] recommended the use of large frequency separations in dual-frequency techniques for future lunar RO missions, given the large measurement noise present in the SELENE radio occultation experiment. SELENE used frequencies of 2218.0000 MHz and 2287.3125 MHz.

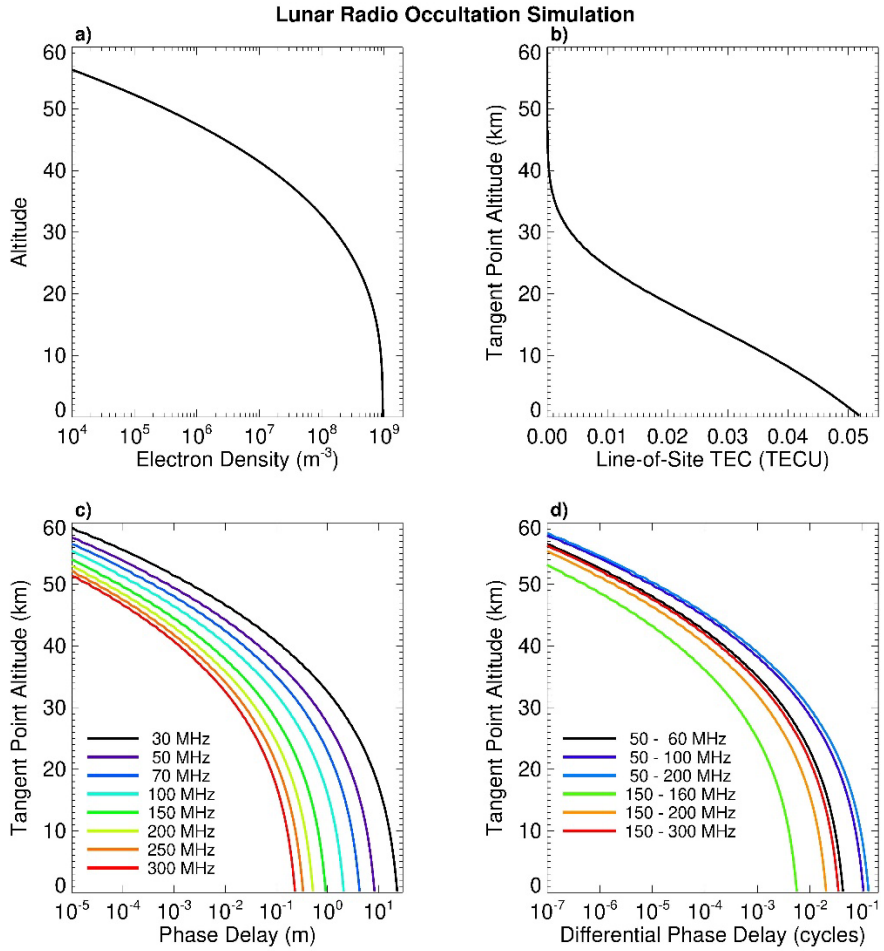

Figure 4. (a) Modeled vertical electron density profile of the lunar ionosphere (Equation 1); (b) Corresponding LOS TEC for the simulated RO event highlighted in Figure 2; (c) Corresponding phase advance along the RO signal path for several test frequencies; (d) Differential phase delay for selected frequency pairs.

4. System and Operational Requirements

For a potential lunar crosslink RO mission, there are a broad range of system and operational considerations including the physical component requirements of an RO system, selection of ideal operating frequencies, atomic clock requirements, measurement sensitivity analysis, orbital considerations, data handling requirements, and cost estimates for a mission life cycle. These aspects would be addressed in a thorough feasibility study. Such a study would cumulatively evaluate the requirements for and feasibility of acquiring high quality and scientifically valuable crosslink RO observations of the lunar ionosphere based on current knowledge of the lunar environment, while evaluating the ideal system parameters with which to do so.

Crosslink lunar RO measurements require at least two distinct orbiting vehicles. The radio receiver and radio transmitter installed in their respective CubeSat payloads must be capable of receiving and transmitting widely (greater than 100 MHz) spaced tones, the tones having a deterministic phase relationship. Both payloads require a highly stable clock source. A preliminary product breakdown structure for a lunar RO mission is shown in Figure 5. The current technology readiness level (TRL) of a lunar RO system is estimated to be level two, based on the International

Organization for Standardization (ISO) 16290:2013 standard [*Heder*, 2017]. A mission concept has been postulated and a technology application has been formulated. The payload technology is stable and well defined for terrestrial use, while the peripheral and supporting sub-systems are expected to be greater than TRL 3. Critical technology elements of an RO system include the clock generator and reference clock assemblies, antenna subsystem and attitude control subsystem.

A feasibility study should include ionosphere RO simulations, which may include numerical raytracing of RO signals across multiple frequencies using a broad range of lunar ionosphere models in order to determine the ideal frequencies for lunar RO. Differential phase delays for a range of test frequencies may be calculated, which would indicate the sensitivity of VHF frequencies for narrowing down the requirements for frequency selection and clock accuracy and stability. In determining ideal frequencies, considerations may include sensitivity to the ionosphere, availability and cost of space-qualified clocks, antenna requirements, and availability of frequency bands. Simulations may also include Doppler shifts due to the relative motion between satellites and satellite line-of-site visibility, which should include satellite attitude control considerations.

The selection of the working frequency range for the RO system is stipulated by the physical characteristics of the lunar ionosphere. The vertical TEC in the lunar ionosphere is several orders of magnitude smaller than that of the Earth's ionosphere [*Reasoner and Burke,* 1972]. *Vyshlov* [1976] demonstrated that the lunar TEC along RO links can reach ~0.03 TECU, with an estimated peak number density of 10^4 cm^{-3} at the lunar surface. However, later studies demonstrated RO TEC that does not exceed 0.015 TECU, with a peak density on the order of 10^2 cm^{-3} [*Imamura et al.*, 2012; *Ando et al.,* 2012; *Choudhary et al.,* 2016]. Integrating vertical density profiles obtained by the latest studies, the vertical TEC is estimated to reach ~0.001 TECU. The accuracy of the signal phase measurements required to accurately estimate this level of TEC using L-band frequencies (GHz range) would need to exceed 1.3×10^{-12}, which is a limiting factor in the selection of sufficiently stable clocks. Another approach is to use lower frequencies at the expense of enlarging the physical size of the transmitting and receiving antennas. The antenna required for use at VHF/UHF frequencies is nominally larger than the CubeSat unit size and will require engineering effort to fit within size constraints of a dispenser or require effort to develop a mechanical deployment method after satellite deployment. The antenna gain needed to meet link budget requirements is an unknown at the time.

The balance between antenna size and availability of clocks with the required stability for space-based applications suggests that the VHF frequency band would be the optimal choice for lunar RO purposes. For example, at 100 MHz, the clock stability must be $\sim10^{-11}$, which is reachable with the state-of-the-art, space application-ready rubidium atomic clocks [e.g., *GPS World Staff,* 2018]. While clocking solutions that meet the estimated frequency stability requirements exist and are readily available, integrating the clock within the timing subsystem while maintaining its performance, managing environmental impacts to the clock stability, and adhering to volume-mass limitations of the satellite bus adds implementation risk.

The requirements for transmitter and receiver oscillator stability would be assessed in a feasibility study. Requirements for the characteristics of the clock sources are conditioned by the selected frequencies and estimated effects of the lunar ionosphere on the propagating signals, and should be subject to further study. A possibility to measure total electron content with an accuracy of 1×10^{-3} TECU requires the clock stability to be ~0.1 ppb at a VHF frequency of 100 MHz. Study of the available COTS components should be performed. Acquired COTS clock sources may be tested for function, frequency precision, and stability. The associated requirements for clock stability may be calculated based on optimal frequencies determined in RO simulations, and assessment of the viability of the clock sources to operate at these frequencies should be performed. Optimal operation frequencies can be updated based on these viability assessments.

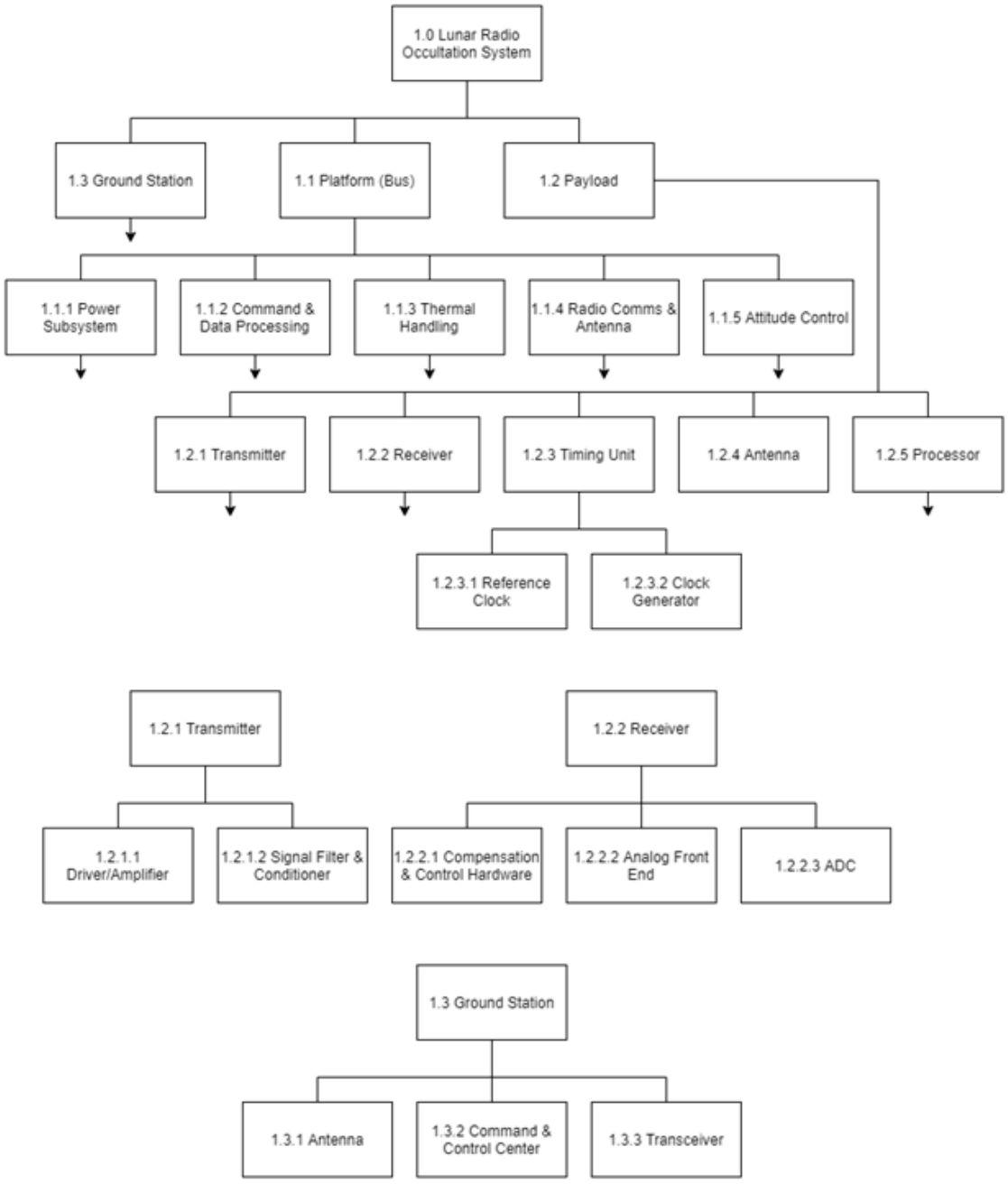

Figure 5. Preliminary product breakdown structure to the assembly level for a potential RIPLIO mission.

Selection of lunar orbits may be based on considerations of lunar orbit stability, accuracy of predicted orbits, ideal distributions of lunar radio occultations, instrument pointing requirements, and launch vehicle selection and trajectory. Orbit simulations may be conducted using software packages such as the Orbit Determination Tool Kit (ODTK) [*Vallado et al.,* 2010], which includes models for the lunar gravity field, solar radiation pressure, and gravitational perturbations of Earth. Lunar gravity field models are based on S- and X-band Doppler data of previous lunar orbiter missions such as Clementine [*Lemoine et al.,* 1997], Lunar Prospector [*Konopliv et al.,* 2001], and the Gravity

Recovery and Interior Laboratory (GRAIL) mission [*Konopliv et al.*, 2014].

Orbital planning should include an appropriate lunar gravity model along with considerations of orbital perturbations (e.g., solar radiation, Earth's gravity), orbital feasibility, orbital lifetime, and maximization of the vertical resolution of RO measurements. The highly unstable lunar orbit requires careful consideration, and the configuration of satellites in lunar orbit is likely to change significantly over time. Lunar orbital lifetimes may range from days to years depending on orbital elements [*Meyer et al.,* 1994]. Fortunately, the nature of the proposed RO satellite constellation allows for continued collection of measurements even as orbits change, and may be a preferable scenario as it would allow for observation of a broader range of lunar regions. Consideration of frozen "resonance" orbits is also a possibility, which can result in more stable orbit configurations and considerably longer orbital lifetimes [*Ely,* 2005; *Lara,* 2011]. Factors that reduce the number of usable orbits are thrust limitations of the CubeSat, fuel requirements for a long-term (greater than one year) mission, and antenna design limitations. The use of specialized plasma thrusters designed for CubeSat propulsion may be considered [*Liang et al.,* 2018].

A current knowledge gap to be addressed in a feasibility study is the limitations of off-the-shelf attitude control subsystems for lunar orbit. Orbiting satellites for lunar RO require strict orientation and coordination, and availability of technology that meets the requirements may affect the TRL of the science instrument and the work required to meet the objectives of a lunar RO mission.

Measurement sensitivity analysis may involve estimation of the link budget for the specific configurations of two or more orbiters, to specify the requirements for the transmitting power and receiver sensitivity. This analysis requires a preliminary model of lunar ionosphere electron density, and a modified ray-tracing algorithm to implement the lunar ionosphere model. Extensive ray-tracing simulations can be conducted using a broad range of frequencies and variable lunar, solar wind, and magnetospheric conditions. The levels of noise of natural (e.g. cosmic background noise) and manmade origins should also be considered, along with associated predictions of uncertainties in simulated ionospheric detections. Analysis may consider the sensitivity of various techniques (e.g., differential phase, differential Doppler) for detecting lunar ionospheric plasma. This process will help in estimation of the power consumption for both the transmitting and receiving parts of the system.

A transmitter capable of broadcasting at more than two frequencies (either simultaneously or interchangeably) may enhance lunar ionospheric observational capabilities, given that the exact range of electron densities within the lunar ionosphere is unknown. This capability would allow for more than one option in frequency pair selection in application of the differential phase technique, thus expanding options for application of optimal frequencies that are most sensitive to the lunar ionosphere under given conditions. This option may be limited by increased signal noise (if broadcasting simultaneously at more than two frequencies), or satellite command limitations (when attempting to switch transmission frequencies).

A lunar RO mission must include comprehensive data processing techniques and algorithms, in order to derive scientifically useful, high level data products from raw RO measurements (e.g., vertical electron density profiles, line-of-site TEC). Existing algorithms for processing Earth-based RO measurements may be adapted to lunar crosslink RO applications. Algorithms can be tested by using results of RO simulations and estimated noise levels, including estimates of uncertainty levels in ionospheric densities and TEC. Optimal sampling rates, vertical resolutions, and measurement integration times can be determined, based on simulation results. Differential phase, differential Doppler, and residual Doppler techniques may be applied in calculation of simulated LOS TEC, with the sensitivity of LOS TEC to each technique analyzed. Techniques to solve for clock and inter-frequency biases may be developed. Techniques to analyze high-level RO data may also be developed, such as data visualization tools and methods to assimilate data into lunar ionosphere models.

5. Relevance to International Science Goals

There has been renewed interest in lunar and deep space exploration in recent years, including development and construction of the Lunar Gateway space station planned for lunar orbit. RIPLIO science objectives directly address several of the planetary science priorities described in Canadian Space Exploration – Science and Space Health Priorities for Next Decade and Beyond: "To understand the role of magnetic fields, plasma and atmosphere/ionosphere dynamics on the history and evolution of planets and other solar system bodies". This science priority specifically targets the "Lunar plasma environment and its regions (PSE-01-03)" as well as "the lunar ionosphere". RIPLIO has the potential to observe the lunar ionosphere with unprecedented detail and from a new perspective by collecting a large number of high-resolution vertical electron density profiles. These measurements would provide capacity to fill in vast gaps in current observational capabilities, including the still unresolved vertical structure of the lunar ionosphere and its variability under sunlight/darkness and a range of solar wind and Earth magnetospheric conditions. Such observations would "unlock the secrets of the lunar ionosphere" and contribute to the "understanding of the Moon and its evolution". Several other research priorities specified in PSE-01-03 can be addressed using potential RIPLIO observations: (1) "Mini-magnetospheres" are thought to interact with the lunar ionosphere [e.g. *Savich,* 1976], and extensive lunar RO observations may provide information integral in the identification and characterization of these structures and their role in the structuring of the lunar ionosphere. (2) RO density profiles near the "lunar terminator" may allow for insight into the unique electrodynamic processes associated with the day-night boundary, including the role of possible enhanced ionosphere densities near the terminator as evidenced by *Hodges et al.* [1974] and *Daily et al.,* [1977]. (3) "Lunar dust and dust storms" may contribute to the formation of ionized dust (e.g. dusty plasma) accompanied by electrons in the lunar ionosphere [*Stubbs et al.*, 2011], with RIPLIO potentially providing a means to statistically characterize the extent and occurrence of electrically charged dust particles. (4) The study of "multi-scale fundamental plasma physics" at the Moon would significantly benefit from extensive lunar ionospheric observations over a wide range of temporal and spatial scales, attainable through a large number of high resolution RO measurements of the lunar ionosphere.

The Artemis lunar program of NASA will include a Lunar Surface Electromagnetics Experiment (LuSEE) [*Bale et al.,* 2020] designed to measure electromagnetic waves on the lunar surface, and will attempt to determine ionosphere density with high accuracy through plasma wave and thermal noise observations. Potential satellite-based RO measurements of RIPLIO would provide a valuable validation tool for such measurements.

The International Lunar Observatory (ILO-1) mission (https://www.iloa.org/mission.html), which involves the Canadian aerospace corporation Canadensys as a prime contractor, is an international collaborative effort to place a lunar astronomy and communications laboratory at the lunar south pole, for the purpose of galactic and astronomical observations and lunar-based communications tests. One possible advantage of lunar-based astronomy is reduced contamination from atmospheric turbulence or dimming, however the "likely effects" of the lunar atmosphere and ionosphere on lunar-based optical observations are unknown [see The National Research Council, The Scientific Context for Exploration of the Moon, pg. 44]. Lunar ionospheric observations, such as those potentially provided by RIPLIO, are thus a critical component of assessing and mitigating the risks posed by the lunar ionosphere on lunar astronomical laboratories such as ILO-1.

Demonstrated feasibility and success of RIPLIO may also open the door for future lunar and planetary crosslink RO missions, including missions involving more than two satellites to provide even greater RO measurement densities. RIPLIO can also potentially act as a testbed for future

missions, providing insight into potential improvements for hardware and software specifications, orbital selections, and chosen transmission frequencies.

6. Summary

This paper presents the concept of a crosslink lunar radio occultation mission, which we call the Radio Instrument Package for Lunar Ionospheric Observation (RIPLIO). The structure and dynamics of the lunar ionosphere are mostly unknown at the present stage. A crosslink lunar RO mission would address the current lack of observational capacity of the lunar ionosphere, providing an unprecedented observational picture of its structure and dynamic behaviour through a broad range of solar wind and magnetospheric conditions. Such observations are required to determine the physical mechanisms governing lunar ionospheric formation and loss, determine its role in the electrodynamics of the near-Moon environment and coupling within the broader environment encompassing the Earth's magnetosphere and ionosphere, and assess the potential safety hazards of the lunar ionosphere for humans and satellite/surface equipment and its potential effects on radio communication and navigation systems. These observations are also essential for development of modeling and predictive capabilities for lunar ionosphere structure and dynamics, and may be integrated into models of the Earth's magnetospheric plasma environment. RIPLIO observations would address several science goals relevant to the renewed interest in lunar and space exploration and potential lunar habitation.

The crosslink radio occultation technique, previously employed in observations of the Martian ionosphere, employs two or more satellites in lunar orbit. From lunar ionosphere density estimates based on limited past observations, lunar ionospheric densities may be calculated from the differential phase of dual-frequency VHF links between two or more satellites in lunar orbit. Simulations of dual-satellite crosslink occultations show 10s of complete RO plasma density retrievals may be obtained per lunar day, depending on orbital configurations. A thorough feasibility study is required to determine the operational and system requirements of a lunar RO mission.

Data Availability Statement

Software written to simulate the lunar ionosphere and crosslink radio occultations and to generate figures is published on Zenodo (Watson, 2022).

References

Abel, N.H. (1826), Auflösung einer mechanischen Aufgabe, *J. Reine Angew. Math.*, 1, 153-157, https://doi.org/10.1515/crll.1826.1.153.

Ando, H., et al. (2012), Dual-spacecraft radio occultation measurement of the electron density near the lunar surface by the SELENE mission, *J. Geophys. Res.*, 117, A08313, https://doi.org/10.1029/2011JA017141.

Andrew, B. H., N. J. B. A. Branson, and D. Wills (1964), Radio observations of the Crab nebula during a lunar occultation, *Nature*, *203*, 171– 173.

Ao, C. O., Edwards, C. D., Kahan, D. S., Pi, X., Asmar, S. W., and Mannucci, A. J. (2015), A first demonstration of Mars crosslink occultation measurements, *Radio Sci.*, *50*, 997– 1007, https://doi.org/10.1002/2015RS005750.

Appleton, E.V.(1932), Wireless studies of the ionosphere, *Journal I.E.E., 71,* 642.

Asmar, S. *et al*. (2016), Demonstration of Mars crosslink occultation measurements for future small spacecraft constellations, *2016 IEEE Aerospace Conference*, Big Sky, MT, 1-6, https://doi.org/10.1109/AERO.2016.7500729.

Bale, S.D., J. W. Bonnell, J. Burns, K. Goetz, J.S. Halekas, D. M. Malaspina, B. Page, M. Pulupa, A.R. Poppe, R. J. MacDowell, M. Maksimovic, A. Zaslavsky (2020), The Lunar Surface Electromagnetics Experiment (LuSEE), *Lunar Surface Science Workshop 2020 (LPI Contrib. No. 2241).*

Benson, J., J.W. Freeman, and H.K Hills (1975), The lunar terminator ionosphere, *Proc. Lunar Sci. Conf., 6th*, *Volume 3,* Houston, Texas, March 17-21, 3013-3021.

Blewitt G. (1990), An automatic editing algorithm for GPS data, *Geophys. Res. Lett., 17,* 199-202, https://doi.org/10.1029/GL017i003p00199.

Brunini, C., Meza, A., Azpilicueta, F. et al. (2004), A New Ionosphere Monitoring Technology Based on GPS, *Astrophysics and Space Science, 290*, 415-429, https://doi.org/10.1023/B:ASTR.0000032540.35594.64.

Choudhary, R. K., Ambili, K. M., Choudhury, S., Dhanya, M. B., and Bhardwaj, A. (2016), On the origin of the ionosphere at the Moon using results from Chandrayaan-1 S band radio occultation experiment and a photochemical model, *Geophys. Res. Lett., 43*, 10,025–10,033, https://doi.org/10.1002/2016GL070612.

Daily, W.D., Barker, W.A., Clark, M.W., Dyal, P., & Parkin, C.W. (1977). Ionosphere and atmosphere of the Moon in the geomagnetic tail. *Journal of Geophysical Research, 82*, 5441-5451, https://doi.org/ 10.1029/JB082I033P05441

Elsmore, B. (1957), Radio observations of the lunar atmosphere, *Philos. Mag.*, *2*, 1040– 1046.

Ely. T.A (2005), Stable Constellations of Frozen Elliptical Inclined Lunar Orbits, *Journal of the Astronautical Sciences, 53*(3), 301-316.

Goto, Y., Fujimoto, T., Kasahara, Y. et al. (2011), Lunar ionosphere exploration method using auroral kilometric radiation, *Earth Planet Sp. 63*, 47–56, https://doi.org/10.5047/eps.2011.01.005.

GPS World Staff (2018), Microsemi debuts chip-scale atomic clock for space, *GPS World*, June 2018.

Hajj, G. A., and Romans, L. J. (1998), Ionospheric electron density profiles obtained with the Global Positioning System: Results from the GPS/MET experiment, *Radio Sci., 33*(1), 175–190, https://doi.org/10.1029/97RS03183.

Halekas, J. S., Delory, G. T., Lin, R. P., Stubbs, T. J., and Farrell, W. M. (2008), Lunar Prospector observations of the electrostatic potential of the lunar surface and its response to incident currents, *J. Geophys. Res.*, 113, A09102, https://doi.org/10.1029/2008JA013194.

Halekas, J. S., Benna, M., Mahaffy, P. R., Elphic, R. C., Poppe, A. R., & Delory, G. T. (2015). Detections of lunar exospheric ions by the LADEE neutral mass spectrometer. Geophysical Research Letters, 42, 5162–5169. https://doi.org/10.1002/2015GL064746

Halekas, J. S., Poppe, A. R., Delory, G. T., Sarantos, M., Farrell, W. M., Angelopoulos, V., & McFadden, J. P. (2012). Lunar pickup ions observed by ARTEMIS: Spatial and temporal distribution and constraints on species and source locations. Journal of Geophysical Research, 117, E06006. https://doi.org/10.1029/2012JE004107

Halekas, J. S., Poppe, A. R., Delory, G. T., Sarantos, M., & McFadden, J. P. (2013). Using ARTEMIS pickup ion observations to place constraints on the lunar atmosphere. Journal of Geophysical Research: Planets, 118, 81–88. https://doi.org/10.1029/2012JE004292

Halekas, J. S., Poppe, A. R., Harada, Y., Bonnell, J. W., Ergun, R. E., & McFadden, J. P. (2018). A tenuous lunar ionosphere in the geomagnetic tail. Geophysical Research Letters, 45, 9450–9459. https://doi.org/10.1029/2018GL079936

Heder, M. (2017). From NASA to EU: the evolution of the TRL scale in Public Sector Innovation (PDF). The Innovation Journal. 22: 1–23. Archived from the original (PDF) on October 11, 2017.

Hernandez-Pajares M., Juan J.M., Sanz J., Orus R., Garcia-Rigo A., Feltens J., Komjathy A., Schaer S.C., Krankoswki A. (2009), The IGS VTEC maps: a reliable source of ionospheric information since 1998, *J. Geod.*, https://doi.org/10.007/s00190-008-0266-1.

Hodges, R.R., J.H. Hoffman, and F.S. Johnson (1974), The lunar atmosphere, *Icarus, 21*(4), 415-426, https://doi.org/10.1016/0019-1035(74)90144-4.

Hodges, R.R. and J.H. Hoffman (1975), Implications of atmospheric Ar escape on the interior structure of the Moon, *Proc. Lunar Sci. Conf., 6th,* Houston, Texas, March 17-21, 3039-3047.

Horányi, M., Sternovsky, Z., Lankton, M. et al. (2014), The Lunar Dust Experiment (LDEX) Onboard the Lunar Atmosphere and Dust Environment Explorer (LADEE) Mission, *Space Sci. Rev., 185*, 93–113, https://doi.org/10.1007/s11214-014-0118-7

Horányi, M. (2016), Summary of the results from the Lunar Dust Experiment (LDEX) onboard the Lunar Atmosphere and Dust Environment (LADEE) Mission, *41st COSPAR Scientific Assembly, abstracts from the meeting that was to be held 30 July - 7 August at the Istanbul Congress Center (ICC), Turkey, but was cancelled.,* Abstract id. C5.2-6-16.

Imamura, T., K.-I. Oyama, T. Iwata, Y. Kono, K. Matsumoto, Q. Liu, H. Noda, Y. Futaana, and A. Nabatov (2008), The possibility of studying the lunar ionosphere with SELENE radio science experiment, *Earth Planets Space, 60*, 387–390.

Imamura, T., et al. (2010), Studying the Lunar Ionosphere with SELENE Radio Science Experiment, *Space Sci. Rev., 154*, 305–316.

Imamura, T., et al. (2012), Radio occultation measurement of the electron density near the lunar surface using a subsatellite on the SELENE mission, *J. Geophys. Res., 117*, A06303, https://doi.org/10.1029/2011JA017293.

Jakowski, N. (2017) "Ionosphere Monitoring", Chapter 39 in *Springer Handbook of Global Navigation Satellite Systems*, edited by P.J.G. Teunissen and O. Montenbruck, published by Springer International Publishing AG, Cham, Switzerland.

Johnson, F. S. (1971), Lunar atmosphere, *Rev. Geophys.*, 9(3), 813– 823, https://doi.org/10.1029/RG009i003p00813.

Komjathy, A., and R. Langley, An assessment of predicted and measured ionospheric total electron content using a regional GPS network, paper presented at Nat. Tech. Meet. Inst. of Nav., Santa Monica, Calif., 22 – 24 January 1996.

Konopliv, A.S., S.W. Asmar, E. Carranza, W.L. Sjogren, and D. N. Yuan (2001), Recent gravity models as a result of the Lunar Prospector mission, *Icarus, 150*(1), 1–8.

Konopliv, A. S., et al. (2014), High-resolution lunar gravity fields from the GRAIL Primary and Extended Missions, *Geophys. Res. Lett.*, *41*, 1452– 1458, https://doi.org/10.1002/2013GL059066.

Lara, M. (2011), Design of long-lifetime lunar orbits: A hybrid approach, *Acta Astronautica, 69*(3-4), 186-199, https://doi.org/10.1016/j.actaastro.2011.03.009.

Lemoine, F.G.R, D.E. Smith, M.T. Zuber, G.A. Neumann, and D.D. Rowlands (1997), A 70th degree lunar gravity model (GLGM-2) from Clementine and other tracking data, *Journal of Geophysical Research: Planets, 102*(7), Article ID 97JE01418, 16339–16359.

Liang, W., C. Christine, R. Luke, S. Alex, S. Kawin, G. Lei, B. Rod, R.-D. Juan (2018), An Integrated RF Power Delivery and Plasma Micro-Thruster System for Nano-Satellites, *Frontiers in Physics, 6*, https://doi.org/10.3389/fphy.2018.00115.

Lin R.P., D.L. Mitchell, D.W. Curtis, K.A. Anderson, C.W. Carlson, J. McFadden, M.H. Acuna, L.L. Hood, A. Binder (1998), Lunar surface magnetic fields and their interaction with the solar wind: results from lunar prospector, *Science 281*(5382), 1480-1484. https://doi.org/10.1126/science.281.5382.1480.

Lindeman, R., Freeman, J. W., Jr., & Vondrak, R. R. (1973), Ions from the lunar atmosphere, *Proceedings of the Lunar Science Conference, 4*, 2889-2896.

McCoy, J.E. (1976), Photometric studies of light scattering above the lunar terminator from Apollo solar corona photography, *Proc. Lunar Sci. Conf. 7th*, 1087-1112.

Meyer, K.W., J.J Buglia, and P.N Desai (1994), Lifetimes of lunar satellite orbits, *NASA Technical Paper 3394,* National Aeronautics and Space Administration, Washington, D.C, 20546-0001.

Mousa, A., and Tsuda, T. (2004), Inversion algorithms for GPS downward looking occultation data: Simulation analysis, *J. Meteorol. Soc. Jpn., 82*(1B), 427-432.

National Research Council (2007), The scientific context for exploration of the moon, Washington DC: The National Academies Press, https://doi.org/10.17226/11954.

Nunn, C., R.F Garcia, Y. Nakamura et al. (2020), Lunar Seismology: A Data and Instrumentation Review*, Space Sci. Rev.*, *216*, 89, https://doi.org/10.1007/s11214-020-00709-3.

Ono, T., Kumamoto, A., Kasahara, Y. et al. (2010), The Lunar Radar Sounder (LRS) Onboard the KAGUYA (SELENE) Spacecraft, *Space Sci. Rev., 154*, 145–192, https://doi.org/10.1007/s11214-010-9673-8.

Pedatella, N. M., X. Yue, and W. S. Schreiner (2015), An improved inversion for FORMOSAT-3/COSMIC ionosphere electron density profiles, *J. Geophys. Res. Space Physics*, *120*, 8942–8953, https://doi.org/10.1002/2015JA021704.

Pluchino, S., F. Schilliro, E. Salerno, G. Pupillo, G. Maccaferri, and P. Cassaro (2008), Radio occultation measurements of the lunar ionosphere, *Memorie della Società Astronomica Italiana Supplement, 12*, 53-59.

Pomalaza-Diaz, J.C. (1967), Measurements of the Lunar Ionosphere by Occultations of the Pioneer 7 Spacecraft, *Stanford Electronics Laboratory Scientific Report No. SU-SEL-67-095*.

Poppe, A. R., Samad, R., Halekas, J. S., Sarantos, M., Delory, G. T., Farrell, W. M., Angelopoulos, V., and McFadden, J. P. (2012), ARTEMIS observations of lunar pick-up ions in the terrestrial magnetotail lobes, *Geophys. Res. Lett., 39*, L17104, https://doi.org/10.1029/2012GL052909.

Poppe, A. R., Fillingim, M. O., Halekas, J. S., Raeder, J., and Angelopoulos, V. (2016), ARTEMIS observations of terrestrial ionospheric molecular ion outflow at the Moon, *Geophys. Res. Lett., 43*, 6749– 6758, https://doi.org/10.1002/2016GL069715.

Reasoner, D.L. and W.J. Burke, (1972), Characteristics of the lunar photoelectron layer in the geomagnetic tail, *J. Geophys. Res., 77*(34), 6671– 6687, https://doi.org/10.1029/JA077i034p06671

Sarantos, M., Hartle, R. E., Killen, R. M., Saito, Y., Slavin, J. A., and Glocer, A. (2012), Flux estimates of ions from the lunar exosphere, Geophys. Res. Lett., 39, L13101, doi:10.1029/2012GL052001.

Savich, N.A. (1976), Cislunar plasma model, *Space res. XVI,* 941-943.

Schreiner, W. S., S. V. Sokolovskiy, C. Rocken, and D. C. Hunt (1999), Analysis and validation of GPS/MET radio occultation data in the ionosphere, *Radio Sci*., *34*(4), 949–966, https://doi.org/10.1029/1999RS900034.

Stern, S. A. (1999), The lunar atmosphere: History, status, current problems, and context, *Rev. Geophys*., https://doi.org/10.1029/1999RG900005.

Stubbs, T.J., Richard R. Vondrak, William M. Farrell (2006), A dynamic fountain model for lunar dust, *Advances in Space Research, 37*(1), 59-66, https://doi.org/10.1016/j.asr.2005.04.048.

Stubbs, T. J., Vondrak, R. R., & Farrell, W. M (2007), Impact of dust on lunar exploration, Workshop on Dust in Planetary Systems (ESA SP-643). September 26-30 2005, Kauai, Hawaii. Editors: Krueger, H. and Graps, A., p.239-243.

Stubbs, T.J., D.A. Glenar, W.M. Farrell, R.R. Vondrak, M.R. Collier, J.S. Halekas, G.T. Delory (2011), On the role of dust in the lunar ionosphere, *Planetary Space Sci., 59*(13), 1659-1664, https://doi.org/10.1016/j.pss.2011.05.011.

Vallado, D., R.S. Hujsak, T.M. Johnson, J.H. Seago, and J.W. Woodburn (2010), Orbit Determination Using ODTK Version 6, *Proceedings of the European Space Astronomy Centre, Madrid, Spain, 3-6 May 2010.*

Vasil'ev, M. B., V. A. Vinogradov, A. S. Vyshlov, O. G. Ivanovskii, M. A. Kolosov, N. A. Savich, V. A. Samovol, L. N. Samoznaev, A. I. Sidorenko, A. I. Sheikhet, and D. Ya. Shtern (1974), Radio transparency of circumlunar space using the Luna-19 station, *Cosmic Res., 12*, 102–107.

Vyshlov, A. S. (1976), Preliminary results of circumlunar plasma research by the Luna 22 spacecraft, *Space Res., 16,* 945–949.

Vyshlov, A. S. and N. A. Savich, Observations of radio source occultations by the moon and the nature of the plasma near the moon, *Cosmic Res., 16,* 450–454, 1979.

Watson, C. (2022). Lunar crosslink RO simulation software: Version 1.0.0 [Software]. Zenodo. https://doi.org/10.5281/zenodo.721592.

Watters, T.R., R.C. Weber, G.C. Collins et al. (2019), Shallow seismic activity and young thrust faults on the Moon, *Nat. Geosci., 12*, 411–417, https://doi.org/10.1038/s41561-019-0362-2.

Zhou, X.-Z., Angelopoulos, V., Poppe, A. R., and Halekas, J. S. (2013), ARTEMIS observations of lunar pickup ions: Mass constraints on ion species, J. Geophys. Res. Planets, 118, 1766- 1774, doi:10.1002/jgre.20125.